



Power Electronic Systems
Laboratory

© 2012 IEEE

Proceedings of the International Conference of Integrated Power Electronics Systems (CIPS 2012), Nuremberg, Germany,
March 6-8, 2012

Electromagnetic Modeling of EMI Input Filters

I. Kovacevic,
A. Müsing,
T. Friedli,
J. W. Kolar

This material is published in order to provide access to research results of the Power Electronic Systems Laboratory / D-ITET / ETH Zurich. Internal or personal use of this material is permitted. However, permission to reprint/republish this material for advertising or promotional purposes or for creating new collective works for resale or redistribution must be obtained from the copyright holder. By choosing to view this document, you agree to all provisions of the copyright laws protecting it.



Eidgenössische Technische Hochschule Zürich
Swiss Federal Institute of Technology Zurich

Electromagnetic Modeling of EMI Input Filters

Dipl.-Ing. Ivana Kovačević, Power Electronic Systems Laboratory, ETH Zürich, Switzerland
 Dipl.-Phys. Andreas Müsing, Power Electronic Systems Laboratory, ETH Zürich, Switzerland
 Dr.-Ing. Thomas Friedli, Power Electronic Systems Laboratory, ETH Zürich, Switzerland
 Prof. Dr. Johann. W. Kolar, Power Electronic Systems Laboratory, ETH Zürich, Switzerland

Abstract

The paper summarizes a new modeling procedure for 3D virtual design of EMI filter circuits. The proposed method, based on the coupling of the Partial Element Equivalent Circuit (PEEC) and Boundary Integral Method (BIM) methods, extends the standard PEEC approach for modeling in the presence of magnetic materials, hence allowing the PEEC-based modeling of toroidal EMI filter inductors. The PEEC-BIM coupled method is implemented into a 3D CAD PEEC-based virtual prototyping platform (*GeckoEMC*). The developed EM simulation tool can give a comprehensive understanding of EM behaviour of EMI filter inductors and capacitors, taking their geometrical and material properties into account. Furthermore, it enables the modeling of optimal EMI filter structures including both parasitics and the effects originating from the mutual coupling and the interconnection of filter elements. The approach is verified by impedance and transfer function measurements of different single phase single-/two- stage EMI filter structures. Good agreement between the measurement and the PEEC-based simulation results was achieved for the frequency range from DC up to 30 MHz.

1 Introduction

With increasing switching frequency and high power density of Power Electronic (PE) systems, the problem to satisfy simultaneously power conversion performance and Electromagnetic Compatibility (EMC) requirements as defined by EMC standards for radiated and conducted emissions [1], is getting more difficult. Today, the design of PE converter systems concerning EM Interference (EMI) problems is mostly based on a trial-and-error process and often demands great knowledge and experience in the wide field of electromagnetics. Accordingly, virtual prototyping is increasing in importance as it enables engineers to obtain comprehensive insight into the electromagnetic behaviour of a PE converter system prior to building the final hardware prototype.

To reduce EMI problems of High Frequency (HF) switched power converters, which typically result from “bad” PCB layouts, components’ parasitics, and mutual electromagnetic coupling, EMI input filters and shielding measures are employed in practice. The necessity of employing EMI input filters is due to conducted noise, which cannot be controlled by proper layout techniques and shielding only. Apart from being an essential part of the power converter, EMI filters introduce additional volume and cost to the overall converter design and therefore have to be properly designed and built [2]. The main aim of the work presented in this paper is to develop an EM simulation environment – *GeckoEMC* [3] – that facilitates virtual prototyping of EMI input filters for power converters.

Low-pass passive filters are commonly used for controlling HF conducted noise. The HF performance of the passive filter components and their PCB arrangement have to be taken into account in order to achieve the necessary attenuation within the whole frequency range of interest

i.e. from 150 kHz to 30 MHz [3]. The real characteristics of components can be modeled by lumped equivalent circuits which are derived from the components’ physical performance. However, the lumped equivalent circuits do not fully explain the electromagnetic coupling effect and more sophisticated modeling techniques have to be used. The Partial Element Equivalent Circuit (PEEC) method represents a useful EM modeling technique for power electronics applications that can be defined as circuit-field coupled problems. The research presented in this paper is based on the PEEC method extended for modeling in the presence of magnetic materials i.e. PEEC-Boundary Integral (PEEC-BIM) coupled method [5], [6]. Specifically, the PEEC-BIM method is developed to enable PEEC-based modeling of toroidal inductors of EMI filters and the paper summarizes the experimental verification results for several single-phase EMI filter structures which were fully modeled and simulated by the proposed method.

2 PEEC-based Modeling of Power Electronic Systems

The enormous increase of computational power of personal computers in recent decades has facilitated the development of EMC simulators based on different numerical techniques, such as Finite Element Method (FEM), Finite Difference Time Method (FDTM), Boundary Element Method (BEM), PEEC, Method of Moments (MoM), etc. [7]. These numerical techniques are derived either from the differential or integral formulation of Maxwell’s equations, in the time or frequency domain. The selection of the right model depends mainly on the application and one can only discuss about the relative (dis)advantages of the specific method, concerning calculation time, accuracy, and implementation complexity [8].

For EMC problems in power electronics, the modeling method of choice is usually the PEEC method [9], [10]. The PEEC method is originally derived for the EM modeling of IC interconnections. It is based on the discretization (i.e. meshing) of electrical conductors into partial elements, i.e. inductance, capacitance, resistance, and voltage/current sources [11]. Thus, it can be easily coupled to any circuit simulator as e.g. *SPICE* or *GeckoCIRCUITS* [12] and solved both in the time and frequency domain. In comparison to the FEM approach, the discretization of the surrounding air volume is not required and only the meshing of conducting, dielectric, and magnetic volumes has to be performed. Accordingly, the PEEC method turns out to be a fast and accurate modeling approach for the circuit-field coupled problems such as PCB tracks, EMI filters, power converter systems, etc. In Fig. 1, the PEEC model of a $0.35\mu\text{m}$ PCB copper track is shown. Starting from the real 3D geometry, the PEEC partial elements (R_L , L , C , V_L , V_C) are first extracted by means of a filament mesh [13], then the PEEC equivalent circuit is derived from Kirchhoff's current and voltage laws, and finally solved for the unknown voltages and currents, $[V, I]$ (c.f. Fig. 1, I_{AB} , V_A , V_B). The voltage sources V_L and V_C in Fig. 1 include mutual inductive couplings between PEEC volume cells and mutual capacitive couplings between PEEC surface cells.

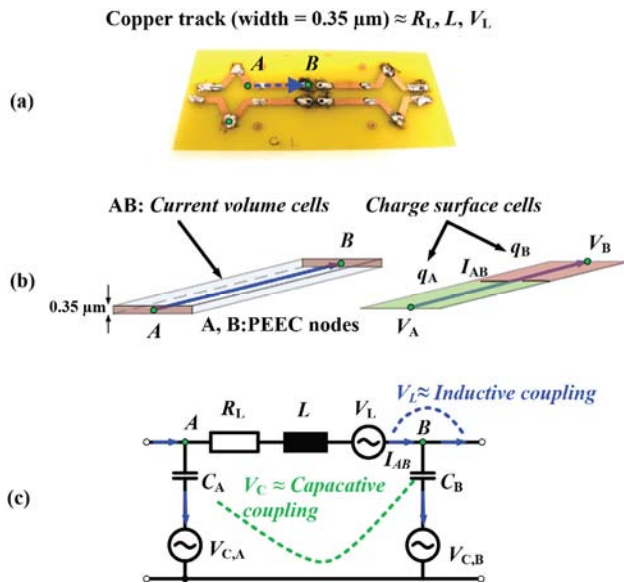


Figure 1 PEEC-based modeling example (a) a $0.35\mu\text{m}$ PCB copper track (b) PEEC model of the PCB track (c) PEEC equivalent circuit of the PCB track.

The PEEC system matrix in the frequency domain is given by

$$\begin{bmatrix} \mathbf{A} & -(\mathbf{R} + j\omega\mathbf{L}) \\ (j\omega\mathbf{P}^{-1} + \mathbf{Y}_L) & \mathbf{A}^T \end{bmatrix} \begin{bmatrix} \mathbf{V} \\ \mathbf{I} \end{bmatrix} = \begin{bmatrix} \mathbf{V}_S \\ \mathbf{I}_S \end{bmatrix}, \quad (1)$$

where \mathbf{A} is the connectivity matrix defining the connection between PEEC partial elements, \mathbf{R} is the resistance diagonal matrix, \mathbf{L} is the inductance matrix consisting of

the self- and mutual inductances between PEEC volume cells, $\mathbf{C} = \mathbf{P}^{-1}$ is the capacitance (potential) matrix defining the self- and mutual- potentials of PEEC surface cells, \mathbf{Y}_L is the admittance matrix consisting of matrix stamps of additional circuit elements connected between PEEC nodes, and \mathbf{I}_S and \mathbf{V}_S are current and voltage sources for modeled excitations. Optionally, magnetic and electric field strengths can be calculated in a post-processing step via the known distribution of the current \mathbf{I} and voltage potentials \mathbf{V} .

2.1 PEEC Modeling in the Presence of Magnetic Materials

The main difficulty of the PEEC method is the inclusion of models for magnetic materials. The PEEC-based modeling of nonlinearity, anisotropy, and other magnetic properties is not straightforward and is not performed in practice. As a result, exact 3D PEEC-based models of magnetic components are not possible and the FE method is typically applied for this class of problems.

As the PEEC method is a linear approach, in order to model magnetic PE components via the PEEC method, the homogenization method has to be used, which means that the magnetic core is modeled as a homogenous and linear material defined by the relative permeability coefficient μ_r . Since the practical design of inductors and transformers is based on frequency dependent $\mu_r(f)$ curves given by manufacturers, or on $\mu_r(f)$ measurements, the homogenization assumption is fully justified for PE applications which simplifies the PEEC-based modeling of magnetic PE components in the frequency domain. Specifically, the EM influence of a magnetic core can be modeled by replacing the core with a fictitious distribution of magnetic currents, \mathbf{K}_M , which have to be further coupled to the electric (excitation) currents. According to EM theory, the coupling between the fictitious magnetic currents and the electric currents is derived from the boundary condition for the tangential component of magnetic field lines (\mathbf{H}_t). Consequently, the PEEC system matrix in the presence of magnetic cores has to be extended by additional columns and rows i.e. \mathbf{a}_{MM} , λ_{MI} and \mathbf{L}_M matrices, to calculate these unknown \mathbf{K}_M currents (2).

$$\begin{bmatrix} \mathbf{A} & -(\mathbf{R} + j\omega\mathbf{L}) & j\omega\mathbf{L}_M \\ (j\omega\mathbf{P}^{-1} + \mathbf{Y}_L) & \mathbf{A}^T & \mathbf{0} \\ \mathbf{0} & \lambda_{MI} & \mathbf{a}_{MM} \end{bmatrix} \begin{bmatrix} \mathbf{V} \\ \mathbf{I} \\ \mathbf{K}_M \end{bmatrix} = \begin{bmatrix} \mathbf{V}_S \\ \mathbf{I}_S \\ \mathbf{0} \end{bmatrix} \quad (2)$$

The \mathbf{L}_M matrix includes the mutual inductances between PEEC volume cells (e.g. electrical conductors) and the magnetic currents \mathbf{K}_M . The elements of \mathbf{a}_{MM} and λ_{MI} matrices are calculated via the boundary conditions (\mathbf{H}_t) that have to be satisfied at the points of the magnetic core surface. The \mathbf{H}_t boundary condition for a point at the core surface with the normal vector \mathbf{n}_{Mk} , is defined by (3a) and then can be further translated in the matrix form as in (3b). The matrix entries of \mathbf{a}_{MM} and λ_{MI} are derived from the Biot-Savart law considering the conductors and \mathbf{K}_M currents as sources of magnetic field. Hence, the new ad-

ditional PEEC elements are defined by the discretization of the magnetic surface into N_M panels carrying the unknown currents \mathbf{K}_{Mk} , $k = 1 \dots N_M$.

$$(\mathbf{H}_{coil(Mk)} + \mathbf{H}_M(Mk)) \times \mathbf{n}_{Mk} = (1 + \frac{1}{\mu_r - 1}) \mathbf{K}_M(Mk) \quad (3a)$$

$$\Rightarrow \lambda_{MI} \cdot \mathbf{I} + \alpha_{MM} \cdot \mathbf{K}_M = 0 \quad (3b)$$

2.2 Literature Overview

The extended PEEC method for modeling in the presence of magnetic materials based on the magnetic current approach is basically explained in [14] and is also used to derive the so called ‘‘MagPEEC’’ method in [15], [16] for RF inductors. Even though the theoretical background of the magnetic current approach is well-known from electromagnetic theory, the difficulties arise with the numerical implementation of the extended PEEC method for the standard PE magnetic component geometries, i.e. the mesh of magnetic volume, the selection of basis-functions for the numerical implementation, and the singularity problem for the calculation of the α_{MM} matrix diagonal elements.

So far, in literature, several assumptions were introduced in order to circumvent these problems for EMI filter inductors. In [17], the authors used a correction factor of an effective permeability to extract the PEEC differential mode partial inductance L_{DM} of a common mode (CM) filter inductor. In [18] and [19], the authors ignore the presence of the magnetic core in order to simplify the PEEC-based model of CM inductors with the aim to perform fast EMC optimization of a power converter.

Accordingly, the research presented in [5], [6], and [20] has been focused on the derivation and implementation of the PEEC-BIM coupled method for complete modeling of EMI filter toroidal inductors characterized by a frequency dependent permeability $\mu_r(f)$. In the following sections it is shown in more detail that the developed method enables fast and accurate simulation of full 3D EMI filter structures. As a result, an EMC simulation tool for virtual prototyping of EMI filters and other power electronic systems, *GeckoEMC*, has been developed.

3 3D Modeling of Filter Components

The starting point for PEEC-based modeling of a full EMI filter structure is the development of 3D PEEC-based models of passive filter components. PEEC models are extracted from the 3D geometry of components, adjusting the input parameters so that a good matching between the simulated and the measured electrical properties of the component is achieved. Subsequently, the correct modeling of the mutual coupling effect is then verified by transfer function measurements.

3.1 Conductors Modeling

In the first approach, two types of conductor geometries are used: rectangular and cylindrical, corresponding to the 3D PEEC models of a PCB track and a solid wire. The input parameters to be defined are the cell conductivity, PEEC cell position, geometry, and discretization numbers.

The 3D PEEC models of a PCB track and a solid wire, shown in Fig. 2, are characterized by the same geometrical and material properties as the real conductors. As the thickness of PCB tracks (height = 0.35 μm) is much less than the other two PCB track dimensions (x and y), the discretization of the PEEC cell in z -direction (c.f. Fig. 2) can be neglected. The x - and y -discretizations of a rectangular PEEC cell and the x - and r -discretizations of a cylindrical volume cell allow for more accurate EM modeling levels, e.g. a more detailed calculation of eddy-currents and the proximity effect.

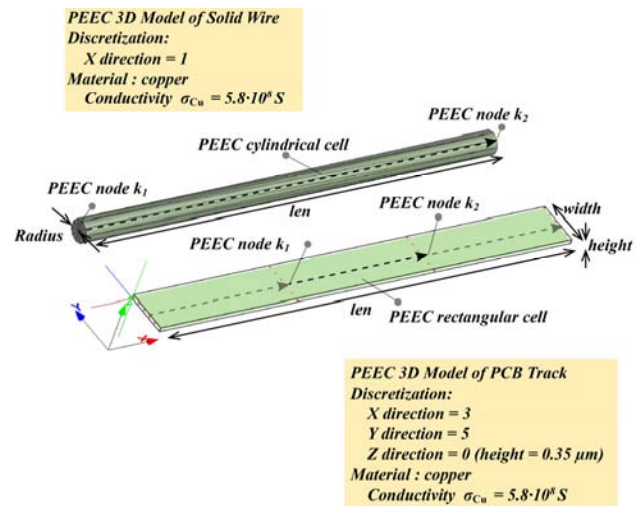


Figure 2 PEEC modeling of a PCB track and a solid wire in *GeckoEMC*.

3.2 X/Y Filter Capacitors Modeling

The homogenization method [21] is applied to model X/Y film filter capacitors. The complex inner structure of a film capacitor is characterized by a rectangular PEEC cell with unknown conductivity ρ , and the same dimensions as the real capacitor. In Fig. 3, the PEEC model of a X/Y film capacitor for EMI noise suppression is presented. The discretization of the PEEC cell is performed in the direction of the current path between positive and negative electrodes (y -direction). The inner PEEC nodes are used to model a frequency-dependant non-uniform current distribution between two electrodes (c.f. Fig. 4). The lumped equivalent circuit of filter capacitors consists of the equivalent series inductance ESL , the equivalent series resistance ESR and the capacitance C . The conductivity ρ and the length of the connectors, len_C , corresponding to respective ESR and ESL , have to be chosen so that the simulated impedance fits accurately the measured impedance characteristics of the capacitor, Z_C .

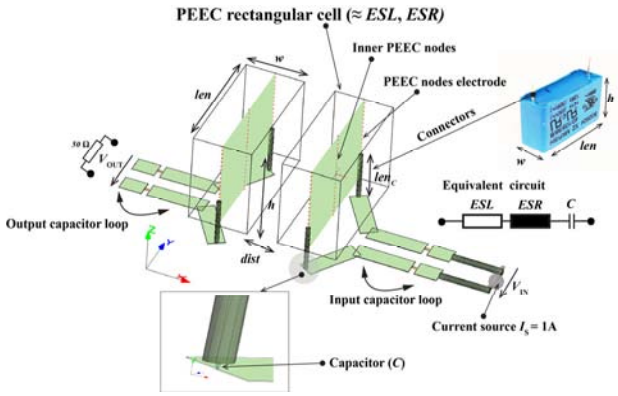


Figure 3 The PEEC-based model of X/Y film capacitors.

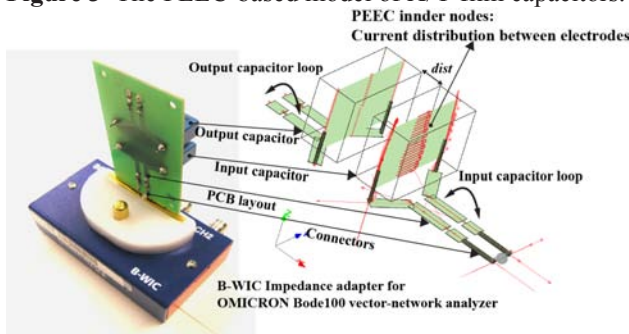


Figure 4 Experimental verification of impedance and mutual coupling effects between the input and output capacitor loops.

The circuit with two capacitor loops presented, in Fig. 3 and Fig. 4, is used to verify the PEEC simulation results for impedance and mutual coupling effects. It can be shown by both, the PEEC simulation and the measurements, that the connectors’ length len_C has a significant influence on the HF behaviour of a capacitor, i.e. ESL . Therefore, the best way to determine the actual length of the connectors is to fit the measured impedance of the input capacitor loop consisting of a capacitor and the PCB tracks. In this way, the PEEC capacitor model is correctly parameterized and can be directly used for further modeling. The output capacitor loop is in that case an open circuit. The mutual coupling is evaluated by simulating the induced voltage in the output capacitor loop terminated with a 50Ω resistance. The simulation results are then compared to the transfer function measurements ($Att = V_{OUT} / V_{IN}$) between the input and output ports. The impedance and transfer measurements were performed using a Bode100 vector-network analyzer from OMICRON (c.f. Section 4.1) operating in the frequency range from $f = 10$ Hz to 40 MHz. The good agreement between the measurements and the PEEC simulation is presented in Fig. 5 for two EPCOS B32924 $1.0 \mu\text{F}$ capacitors at a distance of $dist = 5$ mm. The capacitors, specified in Table 1, are used for the verification.

3.3 Toroid Filter Inductors

The 3D PEEC-based model of toroidal inductors is derived via the PEEC-BIM coupled method, by replacing the magnetic core with a distribution of fictitious magnet-

ic surface currents \mathbf{K}_M , as depicted in Fig. 6. In the case of linear and homogeneous cores, the magnetic current volume density is zero [22]. Hence, only the surface of the core is discretized into N_M panels carrying the unknown currents \mathbf{K}_{Mk} , $k = 1 \dots N_M$. The simulation and measurement results showed that the developed PEEC-model can be simplified by merging together all panels at the angle θ (c.f. Fig. 6) into a magnetic current loop I_{M0j} , $j = 1 \dots n_{div\theta}$, where $n_{div\theta}$ is the discretization number in θ -direction. Therefore, in the presence of a magnetic core the number of unknowns is only $n_{div\theta}$ instead of N_M . The input parameters for the PEEC simulation are the winding properties (number of turns, wire dimensions, wire conductivity) and the core properties (core dimensions and relative permeability curves).

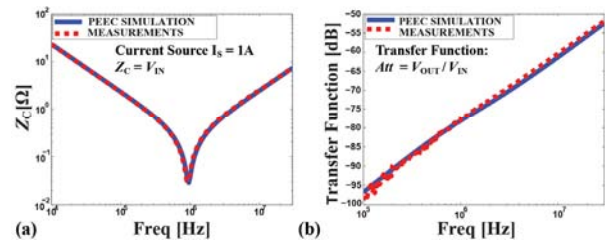


Figure 5 PEEC-based simulation vs. measurements of (a) the input capacitor loop impedance Z_C (b) the transfer function between the input and output capacitor loops.

	Manufacturer, Type, Lead spacing	C [nF]
1	EPCOS, X2 305 V AC, 22.5 mm	470, 680 1000
2	EPCOS, X2 305 V AC, 27.5 mm	680, 1000
3	MURATA, X1/Y1 250 V AC, 10 mm	4.7

Table 1 The main parameters of capacitors used for the verification of the proposed PEEC-based simulation approach.

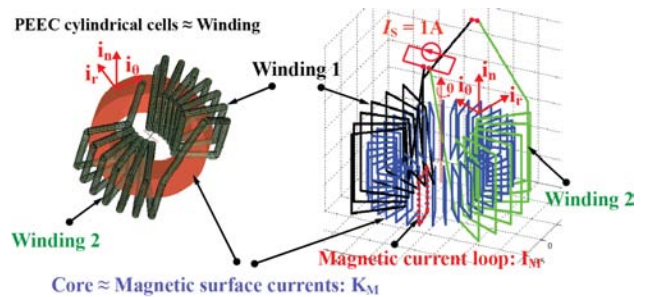


Figure 6 PEEC-BIM model of a single-phase CM inductor with DM winding configuration in *GeckoEMC*.

Furthermore, it was shown that the excitation currents (phase windings) determine the distribution of the magnetic surface currents \mathbf{K}_M around the core i.e. the \mathbf{K}_M strength is higher at the parts of the core covered with the windings. The PEEC-BIM model of a toroidal inductor is verified by the impedance and the near-field measurements of a single-phase common mode (CM) inductor.

The properties of the toroidal inductors used for the verification are summarized in Table 2.

No.	Core: Manufacturer, Type, Material	Winding: turns, wire diameter
1	VAC, VITROPERM 500F W380, nanocrystalline [23]	2 × 7, 1.4 mm
2	Micrometals, T94-26, iron powder [24]	1 × 12, 1.4 mm
3	Magnetics, HighFlux 58204, iron powder [25]	1 × 8, 1.4 mm

Table 2 The inductors used for the verification of the proposed PEEC-based simulation approach.

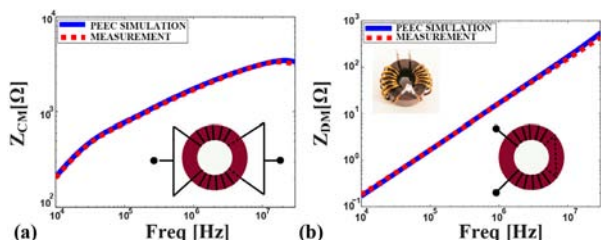


Figure 7 PEEC-BIM simulation vs. measurements of single-phase common mode inductors (c.f. Table 2, core no. 1) (a) CM and (b) DM winding configurations.

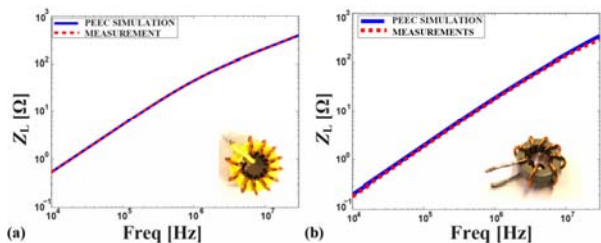


Figure 8 PEEC-BIM simulation vs. measurements of differential mode inductors (c.f. Table 2, core no. 2/3) (a) T94-26 core, 1 × 12 turns (b) HighFlux 58204 core, 1 × 8 turns.

By measuring the mutual coupling between a pick-up coil and a single-phase CM inductor with DM windings configuration, the EM influence of the core can be evaluated as it was shown in [5]. The verification results for the CM and DM impedances of a single-phase CM inductor and for the impedance of DM inductors are presented in Fig. 7 and Fig. 8.

4 Results Verification

The good agreement between the measurements and the PEEC-based simulation results presented in the previous section points out the usefulness of the implemented PEEC-BIM coupled method for 3D modeling of full EMI filter structures. Accordingly, to demonstrate the capabilities of the proposed approach, the transfer function measurements of several single-phase single-/multi-stage EMI filters were performed and then compared to the corresponding PEEC-based simulations in *GeckoEMC*.

4.1 Measurement Setup

As a first step, special attention is directed to building a “good” EMI measurement set-up in order to perform transfer function measurements with minimal external disturbance. In the HF range from approximately 10 MHz onwards measurement results are very sensitive to any parasitic or EM noise coming from other devices and the measurement equipment itself. To investigate the influence of the measurement equipment, two devices operating in different frequency ranges were used: (a) Agilent HP4396A network analyzer with an operating frequency range from $f = 100$ kHz to 1.8 GHz, and (b) OMICRON Bode 100 vector network analyzer, with an operating frequency range from $f = 10$ Hz to 40MHz. The measurement set-ups are schematically presented in Fig. 9.

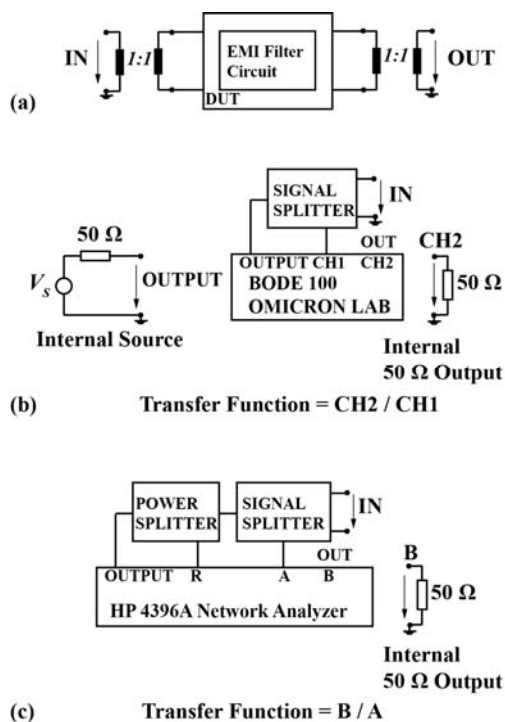


Figure 9 Measurement set-ups: (a) a (DUT) device under test with the connections to (b) Bode 100 vector-network analyzer and (c) HP4396A network analyzer.

The “EMI Filter Circuit” block represents the Device Under Test (DUT) including the passive filter components placed onto the PCB. BNC connectors and 50 Ω coaxial cables are used for the connection between the DUT and the measurement equipment. To match the 50 Ω output resistance of the measurement equipment, 50 Ω resistors are either added onto PCB layout as SMD components or directly soldered to the input/output DUT terminals in series to the signal path. The 50 Ω input resistors are also required in the case of low HF input impedance in parallel to the signal power source.

The 1:1 input and/or output transformers have to be employed for galvanic isolation between the input and output sides to prevent short-circuiting the series impedance in the ground path across the measurement equipment and

also to reduce the shield currents in the coaxial cables. These transformers are not needed for the common-mode measurements with the ground plane directly connected to DUT.

In the PEEC simulation, the transformers are modelled as ideal elements. The 1:1 transformers should have a low impact on the measured frequency characteristics of DUT. As a transformer is typically designed for a special application, its ideal EM behaviour is restricted to a fixed frequency range so that the measurements above and/or below certain frequencies are prone to errors. Specifically, it was observed that both design and position of the transformer can have an impact on the transfer function measurements, which is useful to gain knowledge for building a “good” measurement environment. Two transformers were used in the measurements: Transformer 1, a commercial wide-band transformer (CoilCraft WB1010-1 [26]) and Transformer 2, a custom-made transformer (10 turns of twisted pair on VITROPERM 500F W914 core, wire diameter 0.2 mm) [23] built with approximately two times lower parasitic capacitance between the primary and the secondary windings (10 pF) than the Transformer 1. The calibration of the measurement devices is performed for the through-connection between *IN* and *OUT* ports to compensate the cable and connection setup effects (Fig. 10).

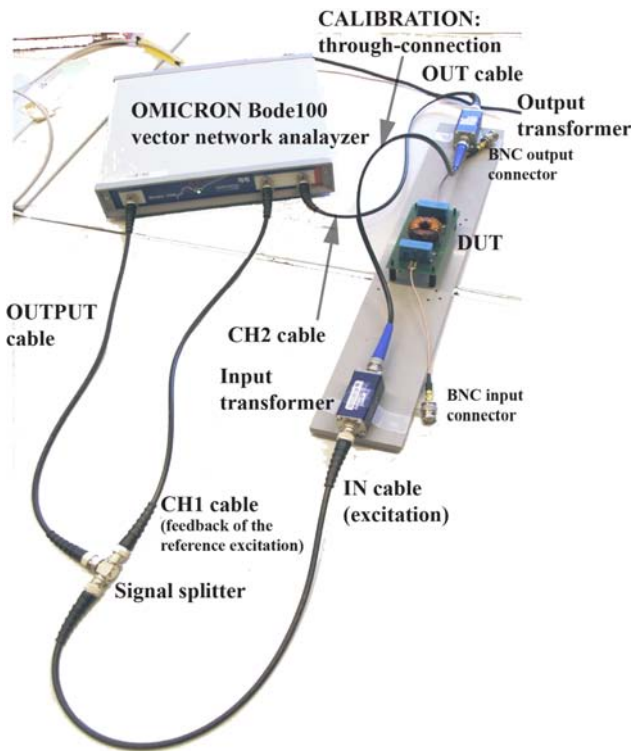


Figure 10 The calibration setup for the OMICRON Bode 100 vector-network analyzer.

4.2 EMI Filter Simulation - Verification

The capabilities of the proposed PEEC modeling approach are verified on the examples of single-/multi-stage single-phase input filter structures. The transfer function measurements are performed for both CM and DM filter configurations (Fig. 11) taking into account also the presence of electrostatic shielding effect. The PCB tracks (width = 3 mm) are implemented on top layer and the copper (ground) plane, *GP*, on the bottom layer of the PCB. When the DM attenuation is measured, the *GP* copper plane behaves as a floating ground plane while for the CM measurements the copper plane *GP* is connected to the ground of the measurement equipment and provides the return path for the CM currents. The leakage inductance of single-phase CM inductors is used as DM inductance for filtering DM current noise.

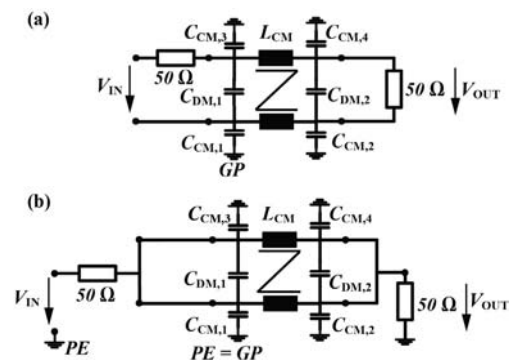


Figure 11 (a) Differential and (b) common mode connection of a single-phase single-stage EMI filter structure.

4.2.1 Modeling of a C-L-C Filter Structure

An example of a *C-L-C* filter structure is presented in Fig. 12 [27].

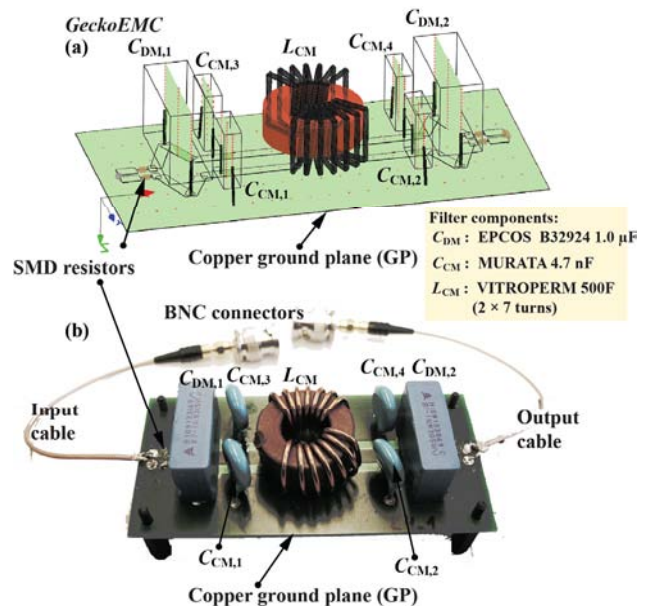


Figure 12 (a) *GeckoEMC* model and (b) practical implementation of a *C-L-C* filter structure with CM capacitors connected to the copper ground plane (*GP*).

The PEEC simulation returns the CM and DM transfer functions which model the measured filter attenuation characteristics observing all resonant frequencies with the accuracy of few dB (Fig. 13).

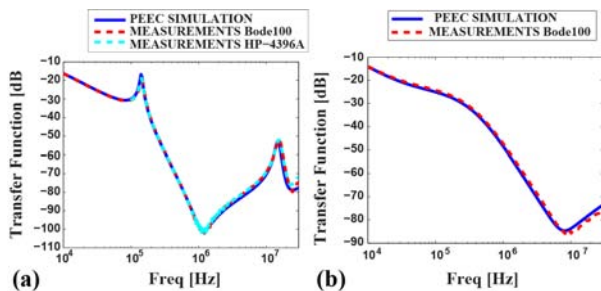


Figure 13 PEEC-simulation vs. measurements of (a) DM and (b) CM transfer functions of the C - L - C filter structure shown in Fig. 12.

The influence of the transformer to the filter output is visible for frequencies above 20 MHz. In Fig. 13, a small mismatch between the measurements and the PEEC simulation of the CM filter transfer function is coming from the inaccuracy of the simulation input parameters such as the core permeability data and geometry of the input connectors. The first resonance frequency at 140 kHz nicely matches with the first resonant frequency of the ideal filter which is due to the resonant circuit formed by $L_{CM,DM} - C_{DM}$; the second resonance at 1.2 MHz results from $C_{DM} - L_{PCB} - ESL(C_{DM})$; and the third resonance at 15 MHz is a result of the currents through the C_{CM} capacitors connected to the copper plane GP . Namely, the PEEC based simulation enables a prediction of EMI filter performance distinguishing the EM influence of all components on the overall EMI filter HF behavior.

4.2.2 Modeling of Electrostatic Shielding Effect

To verify the electrostatic shielding effect, a vertical copper plane connected to the PCB bottom layer via the CM capacitor connections, shown in Fig. 14, is used. Good agreement between the simulation and the measurement (Fig. 15) shows the correctness of the PEEC-based model of conductive thin plates.

According to the results in Fig. 15, the presence of the copper shield increases the attenuation in the HF range that can be explained by the induced eddy-currents in the conductive vertical shield. The transfer function of a C - L - C filter structure with a vertical copper shield and two CM capacitors at the output part was measured to illustrate the influence of the input/output transformers. The first measurement (MEASUREMENT 1) was performed with the custom-made transformer at the input side and the second measurement (MEASUREMENT 2) with the commercial transformer connected at the output side, using the OMICRON Bode 100 network vector analyzer (Fig. 16). In particular, the HF properties of the transformer and its placement introduce approximately ± 5 dB deviation in comparison to the simulation results in the HF range above 10 MHz.

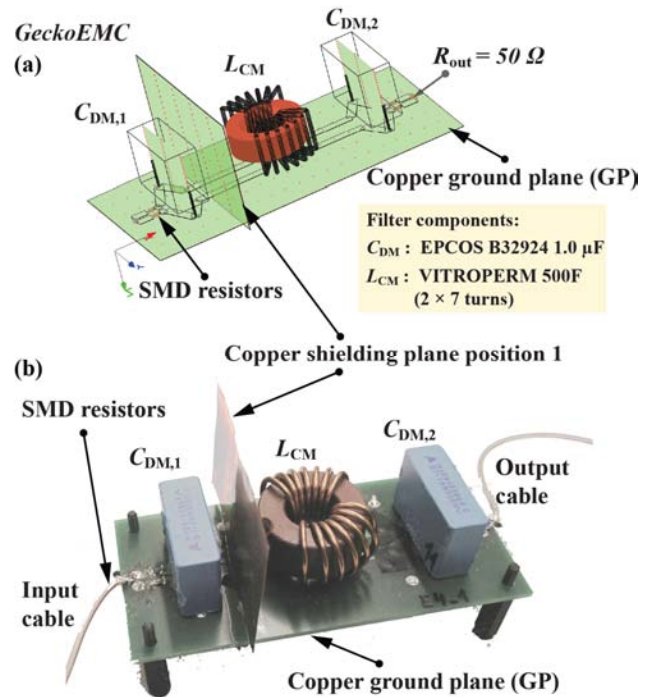


Figure 14 (a) *GeckoEMC* model and (b) practical implementation) of a C - L - C filter structure with an electrostatic copper shield.

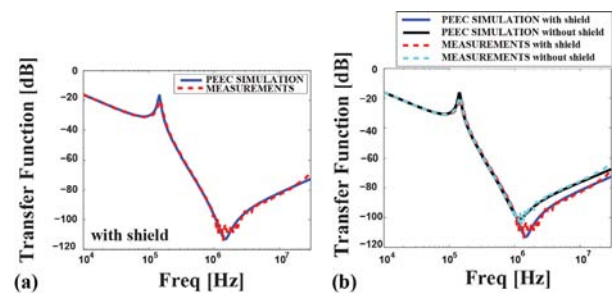


Figure 15 PEEC-simulation vs. measurements of DM transfer functions of the C - L - C filter structure shown in Fig. 14 (a) with and (b) without shielding.

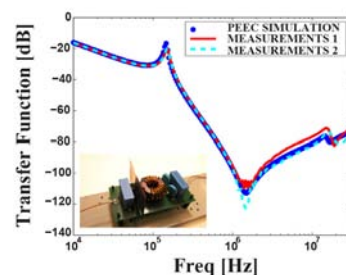


Figure 16 Comparison of two measurements using the OMICRON Bode 100 vector network analyzer.

4.2.3 Modeling of a Two-Stage Filter Structure

The developed PEEC modeling approach is further used to predict the attenuation of a two-stage EMI filter (C - L - C - L - C structure), as shown in Fig. 17 [28]. The comparison between the simulated, the measured (using the Bode 100 analyzer), and the analytical transfer functions are given in Fig. 18. The first order impedance approximation of the DM capacitors (ESL - ESR - C) was used

to analytically calculate the attenuation of a two-stage filter structure. The analytically calculated transfer function deviates from both the measurements and the simulation in the HF range due to the inductive coupling effect of PCB layout which is not included in the analytical filter model. Accordingly, comprehensive analytical circuit modeling requires further measurements like the S-parameters measurements proposed in [29].

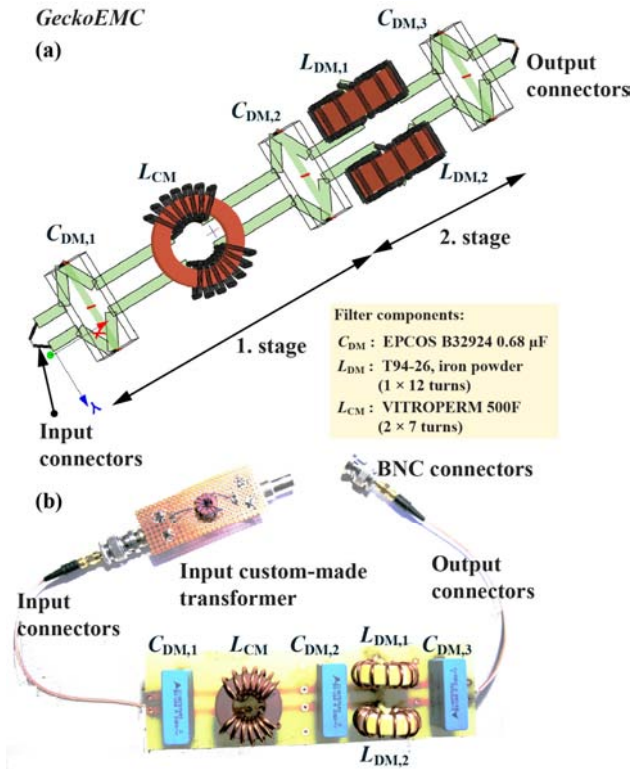


Figure 17 (a) *GeckoEMC* model and (b) practical implementation of a two stage *C-L-C-L-C* filter structure.

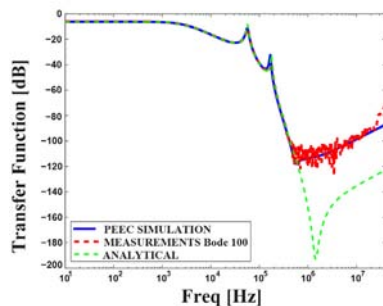


Figure 18 PEEC-simulation vs. measurements of DM transfer functions of the *C-L-C-L-C* filter structure shown in Fig. 17.

Three resonant frequencies in the transfer function can be observed: $f_{R1} = 0.59$ kHz (due to $C_{DM} - L_{DM}$), $f_{R2} = 174$ kHz (due to $C_{DM} - L_{PCB} - L_{CM}$), $f_{R3} = 588$ kHz (due to $C_{DM} - L_{PCB} - ESL$). A replacement of the 3D DM inductor model with a lumped circuit element L [via Y_L see (1)], shows clearly that the inductive coupling between the DM inductors can be neglected and does not change transfer function significantly. This implies that

the dominant coupling effect is actually originating from the PCB layout and the DM capacitors *ESL*. The mismatch above 10 MHz is due to the HF influence of the transformer. The modeled two-stage EMI filter introduces an insertion loss of approximately -120 dB, which is at the limit of the measurement equipment and cannot be accurately measured.

5 *GeckoEMC* Simulation Performance

The mesh of the magnetic surface into N_M panels determines the computational complexity and accuracy of the implemented PEEC-BIM method. The simulations were performed on standard PCs with a 64-bit Win OS and a CPU clock frequency of 2.4 GHz. The PEEC simulations of the filter circuits presented in Section 4 take several minutes depending on the number of magnetic elements i.e. magnetic cores to be modeled. The calculation time can be separated into the pre-calculation of α_{MM} and λ_{MI} matrix elements and the post-calculation e.g. the calculation of transfer function in N_F points in the frequency domain. Thus, the PEEC-based modeling of the two-stage single-phase filter presented in Fig. 17 results in a 1692×1692 square system matrix, and requires a simulation time of 8 min: 6 min for pre-calculation and 2 min for post-calculation in $N_F = 401$ frequency points in the range from $f = 10$ Hz to 40 MHz. The good matching between the measurements and the PEEC-simulation results demonstrate that the PEEC discretization allows accurate 3D modeling of power electronic systems with significantly less computational effort than required for an equivalent FEM analysis.

6 Conclusion

The work presented in the paper enables an efficient virtual design of EMI filters and power converter systems regarding both electrical functionality and EMC design constraints. The PEEC method is shown to be a suitable modeling technique for power electronic applications providing simultaneously time flexibility, speed, and accuracy. In the verification step, good agreement between measurements (accuracy of ± 5 dB) and PEEC-based simulation results of the filter transfer function was achieved for different single-phase single- and /two-stage EMI input filter circuits, used to suppress conducted DM and/or CM noise in the real power electronics systems. The optimal PCB placement and selection of the components is possible by recognizing the critical mutual coupling and parasitics effects. Accordingly, the developed EMC modeling environment (*GeckoEMC*) represents a highly useful tool for virtual prototyping of EMI filters and other power converter systems, speeding up the design process and allowing engineers without wide practical experience to find good EMC designs.

The proposed PEEC-BIM coupled method implemented in *GeckoEMC* allows currently 3D electromagnetic mod-

eling of toroidal inductors. In the course of future research, PEEC-BIM modeling of other core geometries will be examined in more detail.

7 References

- [1] R. Redl, "Electromagnetic environmental impact of power electronics equipment," in Proc. of the IEEE, vol. 89, no. 6, pp. 926–938, June, 2001.
- [2] M. L. Heldwein, "EMC filtering of three-phase power converters," Ph.D. dissertation, Swiss Federal Institute of Technology, Zürich, 2007.
- [3] S. Weber, E. Hoene, S. Guttowski, J. John, and H. Reichl, "Predicting Parasitics and Inductive Coupling in EMI-Filters," in Proc. of 21st Annual *IEEE Applied Power Electronic Conf. and Expo. (APEC)*, Dallas, USA, March 19-23, 2006, pp. 1157-1160.
- [4] Gecko Research, *GeckoEMC*, [Online]: <http://www.gecko-research.com/geckoemc.html>.
- [5] I. Kovacevic, T. Friedli, A. Müsing, and J. W. Kolar, "A Full PEEC Modeling of EMI Filter Inductors in Frequency Domain," presented at 18th *Int. Conf. on the Computation of Electromagnetic Fields (COM-PUMAG)*, Sydney, July 12-15, 2011, pp.
- [6] I. Kovacevic, A. Müsing, and J. W. Kolar, "PEEC modeling of toroidal magnetic inductors in frequency domain," in Proc. of *Int. Power Electronic Conf. (IPEC)*, Sapporo, Japan, July 21-24, 2010, pp. 3158-3165.
- [7] J. Ekman, "Electromagnetic modeling using the Partial Element Equivalent Circuit method," Ph.D. dissertation, Lulea University of Technology, Sweden, 2003.
- [8] H. Kogure, Y. Kogure, and J. C. Rautio, Introduction to RF design using EM simulators, 2010, Artech House Publishers.
- [9] A. Müsing, M. L. Heldwein, T. Friedli, and J. W. Kolar, "Steps towards prediction of conducted emission levels of an RB-IGBT Indirect Matrix Converter," in Proc. of *Power Conversion Conf. (PCC)*, Nagoya, April 2-5, 2007, pp. 1181-1188.
- [10] A. Domurat-Linde and E. Hoene, "Investigation and PEEC based simulation of radiated emissions produced by power electronic converters," in Proc. of 6th *Inter. Conf. on Integrated Power Electronic Systems (CIPS)*, March 16-18, 2010, Paper 13.2.
- [11] H. Heeb and A. Ruehli, "Three-Dimensional interconnect analysis using partial element equivalent circuits," *IEEE Trans. on Circuits and Systems 1: Fundamental Theory and Applications*, vol. 39, no. 11, pp. 974-982, 1992.
- [12] Gecko Research, *GeckoCircuits*, [Online]: <http://www.gecko-research.com/geckocircuits.html>.
- [13] A. Muesing, J. Ekman, and J. W. Kolar, "Efficient calculation of nonorthogonal partial elements for the PEEC method," *Trans. on Magnetics*, vol. 45, no.3, pp. 1140-1143, 2009.
- [14] G. Antonini, M. Sabatini, G. Miscione, "PEEC modeling of linear magnetic materials," in Proc. of *IEEE Int. Symposium on Electromagnetic Compatibility*, Portland, USA, Aug. 14-18, 2006, pp. 93-98.
- [15] H. Long, Z. Feng, H. Feng, et al. "A new modeling technique for simulating 3-D arbitrary conductor-magnetic structures for simulating RFIC applications," *IEEE Tran. on Electron. Devices*, vol. 52, no. 7, pp. 1354-1363, 2005.
- [16] P. Qijun, M. Weiming, Z. Zhihua et al., "MagPEEC modeling technique based on GMD," in Proc of APEMC 2008, Singapore, May 19-23, 2008, pp. 662-665.
- [17] E. Hoene, A. Lissner, S. Weber, S. Guttowski, W. Johan, and H. Reichl, "Simulating electromagnetic interactions in high power density converters," in Proc. of 36th *IEEE Power Electronic Specialists Conference (PESC)*, Recife, Brazil, June 12-16, 2005, pp. 1665-1670.
- [18] T. De Oliveira, J-L. Schanen, J-M. Guichon, and L. Gerbaud, "Automatic layout optimization of an EMC filter," in Proc. of *IEEE Energy Conversion Congress and Expo. (ECCE)*, Atlanta, Georgia, USA, Sept. 12-16, 2010, pp. 2679-2685.
- [19] T. De Oliveira, J-M. Guichon, J-L. Schanen, and L. Gerbaud, "PEEC models for EMC filter layout optimization," in Proc of 6th *Inter. Conf. on Integrated Power Electronic Systems (CIPS)*, March 16-18, 2010, Paper 13.3.
- [20] I. Kovacevic, T. Friedli, A. Müsing, and J. W. Kolar, "PEEC-based virtual design of EMI input filters," in Proc. of *IEEE Energy Conversion Congress and Expo. (ECCE)*, Phoenix, USA, Sept. 17-22, 2011, pp. 1935-1941.
- [21] E. Hoene, "EMC in Power Electronics," in Proc. of 5th *Inter. Conf. on Integrated Power Electronic Systems (CIPS)*, March 11-3, 2008, pp. 1-5.
- [22] D. M. Cook, The theory of the electromagnetic field, 1975, Prentice-Hall, Inc., Englewood Cliffs, New Jersey, pp. 289-324.
- [23] Vacuumschmelze, Nanocrystalline VITROPERM – EMC Components, Vacuumschmelze GmbH. & Co., 2004.
- [24] Micrometals, [Online]:<http://www.micrometals.com>.
- [25] Magnetics, [Online]:<http://www.mag-inc.com>.
- [26] CoilCraft, [Online]: <http://www.coilcraft.com>.
- [27] S. Wang, F. C. Lee, D. Y. Chen, and W. G. Odendaal, "Effects of parasitic parameters on EMI filter performance," *IEEE Trans. on Power Electronics*, vol. 19, no. 3, pp. 869-877, May, 2004.
- [28] Schaffner, *Datasheets: Single Stage Filters*, [Online]: <http://www.schaffnerusa.com/>.
- [29] S. Wang, F. C. Lee, D. Y. Chen, and W. G. Odendaal, "Characterization and parasitic extraction of EMI filters using scattering parameters," *IEEE Trans. on Power Electronics*, vol. 20, no. 2, pp. 502-510, 2005.